Thesis/
Reports
Beier,
P.

Landscape characteristics of Mexican spotted owl habitat

Final Report

Landscape characteristics of Mexican spotted owl habitat

Forest Service Agreement Number 01-JV-11221607-039

Paul Beier, School of Forestry and Merriam-Powell Center for Environmental Research, Northern Arizona University, Flagstaff, AZ 86011, USA

Phone: (928) 523-9341

Email: Paul.Beier@nau.edu

Jeff Jenness, Jenness Enterprises, 3020 N. Schevene Blvd., Flagstaff, AZ 86004, USA (NAU Contract # PC 01BV0001712)

Phone: (928) 607-4638

Email: jeffj@jennessent.com

Website: http://www.jennessent.com

Table of Contents

Introduction 5
Study Area 5
Data 6
Elevation: 7
Slope: 8
Solar Radiation Index: 8
Surface Area Ratio: 11
Road Density: 11
Protection: 12
Methods 13
Results 14
Discussion: 16
Acknowledgments 19
References: 20
Tables: 22
Figures: 27

List of Tables

Table 1: Number of grid cells corresponding to neighborhood sizes 22
Table 2: Proportion of landscape corresponding to all spatial scales of slope values at 90th percentile 23
Table 3: Landscape proportions and owl location proportions of individual grid analyses, showing only those spatial scales with the lowest landscape proportion at each percentile level 24
Table 4: Best models at each Predictive Accuracy Percentile Level, from all possible permutations of best individual grids (see Table 3) 26

List of Figures

Figure 1: We used the Upper Gila Mountains recovery unit for our study area. Our owl locations were taken from randomly-distributed watersheds within this area, and our landscape variables and predictive models encompass the entire area. 27
Figure 2: Solar radiation grids for 10:00 am on three days in the year 2000, shaded from black (cell value = 0), meaning no sunlight hit that cell) to white (cell value = 255, meaning that cell faced the sun directly). We calculated these grids for all hours of the day in which the sun was up on that day, and added them to get daily totals for each of the 12 days of the year. We then added these 12 daily totals and divided the sum by 12 to get a solar radiation grid representing the average amount of daily radiation each cell gets over the entire year. 28
Figure 3: Protection depends on both proximity and height. In this case, Point B is both higher and at a steeper angle from the origin than Point A, yet Point A outscores Point B because it is closer. Using this method, we would conclude that a 300-meter cliff located 200 meters away would offer almost twice as much protection as a 750-meter cliff located 400 meters away (with respective scores of 0.280 and 0.155). This calculation is repeated eight times in eight directions, and the final cell value reflects the average of maximum protection values calculated in the eight directions. 29
Figure 4: Different combinations of height and proximity can produce the same protection values. In this example, a 67-meter cliff 80 meters away offers the same protection value as a 3.6-meter cliff 20 meters away. 30
Figure 5: Proportions of the landscape corresponding with percentile ranges of Elevation values, at 6 spatial scales. 31
Figure 6: Proportions of the landscape corresponding with percentile ranges of Slope values, at 6 spatial scales. 32
Figure 7: Proportions of the landscape corresponding with percentile ranges of Solar Radiation values, at 6 spatial scales. 33
Figure 8: Proportions of the landscape corresponding with percentile ranges of Surface Ratio values, at 6 spatial scales. 34
Figure 9: Proportions of the landscape corresponding with percentile ranges of Road Density values, at 6 spatial scales. 35
Figure 10: Proportions of the landscape corresponding with percentile ranges of Protection values, at 6 spatial scales. 36
Figure 11: Histogram of 355 road density values from the 1000m spatial scale. 37
Figure 12: Landscape proportion and predictive accuracy for all possible combinations of Elevation, Slope, Surface Ratio and Protection layers in which the individual layer predicted $\geq$ 90% of the owl locations correctly. 38
Figure 13: Three of the 25 best models, illustrating the actual landscape predicted to be owl habitat when 77%, 90% and 100% of the owl locations are predicted accurately. 39

Introduction

The Mexican spotted owl (*Strix occidentalis lucida*) occurs in forested mountains and canyonland terrain throughout the southwestern United States and well into Mexico (Ward et al. 1995). This owl is associated with complex late-successional forests throughout much of this range (Ganey and Dick 1995). Because of concerns over the effect of timber harvest on amount and distribution of late-successional forest, the owl was listed as threatened in 1993 (Cully and Austin 1993).

Most studies of Mexican spotted owl habitat relationships (reviewed in Ganey and Dick, 1995) have been restricted in geographic area and/or have focused on fine spatial scales (home-range and below). Few studies have examined landscape-scale habitat characteristics, and those that have focused on nest or roost sites and surrounding areas (Grubb et al. 1997, Peery et al. 1999). Consequently, we have little understanding of how large-scale landscape patterns affect habitat occupancy and demography of Mexican spotted owls, nor do we understand the relative importance of different spatial scales in determining occupancy patterns of owls.

As part of the recovery efforts for this owl, the Rocky Mountain Research Station conducted a pilot study evaluating proposed methods for monitoring population trend of the Mexican spotted owl (Ganey et al. 1999a). This pilot study involved mark-recapture sampling of spotted owls on 25 randomly-located study areas in central Arizona and New Mexico. The sampling design involved completely surveying the 25 study areas, so that inferences could be made about landscapes occupied and not occupied by spotted owls.

This current study was intended to evaluate the influence of road density and topographic landscape variables on occupancy patterns of Mexican spotted owls, using the owl location data collected during that pilot study.

Study Area

Our study area was approximately 54,850 square kilometers in size and encompassed the entire Upper Gila Mountains recovery unit (Figure 1), as described by Rinkevich et al. in the Recovery Plan for the Mexican Spotted Owl (Rinkevich et al. 1995). Detailed information on land use, vegetation patterns and other features of this recovery unit may be reviewed in Rinkevich et al. (1995), but in general this area represents a transition zone between the Colorado Plateau province to the north and the Basin and Range provinces to the south, and is characterized by steep mountains and entrenched river basins dissecting high plateaus (Ganey et al. 1999b).

Data

Owl Location Data (Response Variable): We used owl locations gathered during the 1999 spotted owl monitoring study (Ganey et al. 1999a) to identify those habitat characteristics most used by owls. Within this separate study we identified 47 spotted owl territories located on or near 25 sampling units randomly distributed across the Upper Gila Mountains recovery unit, banded 58 adult or subadult owls, and recorded a large number of owl locations. We decided to analyze only the daytime locations because these were the most accurate, and because we would like to eventually test models derived from these locations with daytime locational data gathered in previous years. Our total owl location dataset comprised 343 daytime observations plus 12 nocturnal observations that were included inadvertently. See Ganey et al. (1999b) for a detailed description of survey methods and results from this study.

Analytic Data Layers (Predictor Variables): We looked for significant habitat characteristics using 5 data layers describing morphological aspects of the Upper Gila Mountains recovery unit landscape (Elevation, Slope, Solar Radiation Index, Surface Area Ratio and Protection) and 1 layer describing road density across the landscape. All landscape morphology data were derived from 15 1 x 1 degree USGS 1:250,000 scale DEMs downloaded from the USGS EROS data center web site (United States Geological Survey 2002), which in the Upper Gila Mountains Recovery Unit have a cell size measuring approximately 92 meters on a side. We converted these DEMs into ArcInfo grids, combined them into a single seamless

grid, and then projected the final grid into the UTM Zone 12 projection using the "Reproject Grids" extension (Quantitative Decisions 1999).

Throughout this report we refer to "grids", and for this report a "grid" is a specific type of geographic data used by ArcInfo and ArcView. A grid is essentially a raster image in which each pixel is referred to as a "cell", and has a particular value associated with it. For the DEMs, the cell value reflects the elevation in meters of the central point in that cell.

For each of these 6 data grids, we generated 6 new grids reflecting the average data value within 6 progressively larger circular neighborhoods surrounding each cell. These circular neighborhoods allow us to examine each data grid at different spatial scales. The 6 neighborhoods had a radius of 1m (meaning the neighborhood grid was equivalent to the original grid), 100m, 200m, 400m, 800m and 1000m. This produced a total of 36 data grids to compare with our owl locations. The number of grid cells used in each neighborhood analysis are described in Table 1:

All 36 data grids covered the entire Upper Gila Mountains recovery unit and consisted of > 6,000,000 cells with data.

Elevation:

These are basic descriptive statistics of elevation within the watersheds.

Elevation Grids (Datasets included on CD 1):

a. Elev_1: Elevation value on the cell

b. Elev_100: Mean Elevation value for all cells with centers ≤ 100 meters of cell center.

c. Elev_200: Mean Elevation value for all cells with centers ≤ 200 meters of cell center.

d. Elev_400: Mean Elevation value for all cells with centers ≤ 400 meters of cell center.

e. Elev_800: Mean Elevation value for all cells with centers ≤ 800 meters of cell center.

f. Elev_1000: Mean Elevation value for all cells with centers ≤ 1000 meters of cell center.

Slope:

We calculated a slope grid in which the value in each cell represents the average slope in degrees for that cell. We used the standard ArcView Slope-generation function, which calculates slope using the following algorithm (quoted directly from the ArcView Spatial Analyst help file for "Slope Discussion" [ESRI 2000a, b]):

> *"Conceptually, the Slope request fits a plane to the z values of a 3x3 cell neighborhood around the processing or center cell. The direction the plane faces is the aspect for the processing cell. The slope for the cell is calculated from the 3x3 neighborhood using the average maximum technique (see references).*
>
> *The actual algorithm that is used to calculate slope is:*
>
> *rise_run = SQRT(SQR(dz/dx)+SQR(dz/dy))*
> *degree_slope = ATAN(rise_run) * 57.29578*
>
> *where the deltas are calculated using a 3x3 roving window, where a through i represent the values in the window:*
>
> *a b c*
> *d e f*
> *g h i*
>
> *(dz/dx) = ((a + 2d + g) - (c + 2f + i)) / (8 * x_mesh_spacing)*
> *(dz/dy) = ((a + 2b + c) - (g + 2h + i)) / (8 * y_mesh_spacing)*
>
> *References: Burrough, P.A., (1986). Principles of Geographical Information Systems for Land Resources Assessment. Oxford University Press, New York, p. 50."*

We then generated neighborhood grids where each cell value represented the mean slope for all those cells whose cell centers lay within the specified distance.

Slope Grids (Datasets included on CD 2):

a. Slop_1: Slope value on the cell

b. Slop_100: Mean slope value for all cells with centers $\leq$ 100 meters of cell center.

c. Slop_200: Mean slope value for all cells with centers $\leq$ 200 meters of cell center.

d. Slop_400: Mean slope value for all cells with centers $\leq$ 400 meters of cell center.

e. Slop_800: Mean slope value for all cells with centers $\leq$ 800 meters of cell center.

f. Slop_1000: Mean slope value for all cells with centers $\leq$ 1000 meters of cell center.

Solar Radiation Index:

This solar radiation index reflects the degree to which each cell in the Upper Gila Mountains recovery unit directly faces the sun.

We calculated a series of grids representing different moments in time in which each cell has a value ranging between 0 and 255, where the value reflects the amount of sunlight hitting that cell at that moment in time. A value of 0 means that no sunlight is hitting that cell at that moment in time (i.e. it is shadowed by a ridge or mountain, or just facing away from the sun). A value of 255 means that that cell is directly facing the sun at that moment in time and absorbing the most sunlight possible. These units do not reflect any standard solar radiation measure but they do accurately represent the relative amount of sunlight hitting any particular area.

For each radiation grid we calculated, we input the bearing and azimuth to the sun for the particular moment in time that grid represented. We used the United States Naval Observatory solar position calculator (U.S. Naval Observatory 2000) to calculate the bearings and angles for each hour of the day when the sun was up, on 12 different days in the year 2000. We selected the 21st of each month in order to capture both the summer and winter solstices (June 21 and December 21) and the vernal and autumnal equinoxes (close to March 21 and September 21), as well as to get a good representation of the solar radiation at any point during the year (Figure 2). We then summed up all the hourly solar radiation grids from each of the 12 days to get daily totals. Each of these daily totals represents the total amount of solar radiation hitting that area during that day. Days during the winter have lower totals because 1) the sun is at a lower angle, and 2) there are fewer hourly grids to add up. Finally we added each of the 12 daily total grids and divided that grid by 12 to get a final solar radiation grid representing the average amount of radiation each cell gets over an entire year.

When using the U.S. Naval Observatory's solar position calculator, we had to enter a longitude and latitude on the planet's surface to calculate from. we assumed that we could take the longitude of a central point in the study area and have that longitude represent the entire study area. The Upper Gila Mountains Recovery unit ranges from 107.1° West to 112.6° West, so we used 110° West as our longitude.

The Upper Gila Mountains Recovery Unit ranges from about 32.7° to 35.6° in latitude, and the amount of solar radiation is affected by the latitude of the point in question. The best way to address this issue would be to use the latitude of each cell when calculating the solar radiation hitting that cell but we could not think of a good way to do this. To try and compensate for the problem, we calculated a solar radiation grid for the entire recovery unit based on a latitude of 35° North, then another grid based on 33° North. We then derived an adjustment factor based on the difference between the two grids at 33° North and applied this adjustment factor to the 35° North grid.

Adjustment Factor Details: We wanted to apply the adjustment factor to the 35° North grid so we made the adjustment factor equal to 1 at 35° Latitude. We then calculated the mean ratio between the two grids at 33° latitude and found that the 33° grid values at 33° Latitude averaged 1.0126 × the 35° values, meaning that our adjustment factor needed to go from 1 (at 35°) to 1.0126 (at 33°). We then generated a grid of adjustment factor values extending over the entire latitudinal range of the Upper Gila Mountains Recover Unit, such that the cell values were equal to:

$$\left(\frac{35 - Cell\ Latitude}{2}\right) \times 1.0126$$

We then multiplied the 35° grid by this adjustment factor grid to get the final solar value grid.

We then generated neighborhood grids where each cell value represented the mean solar radiation value for all those cells whose cell centers lay within the specified distance.

Solar Radiation Grids (Datasets included on CD 3):

a) Sol_1: Solar radiation value on the cell

b) Sol_100: Mean solar radiation value for all cells with centers ≤ 100 meters of cell center.

c) Sol_200: Mean solar radiation value for all cells with centers ≤ 200 meters of cell center.

d) Sol_400: Mean solar radiation value for all cells with centers ≤ 400 meters of cell center.

e) Sol_800: Mean solar radiation value for all cells with centers ≤ 800 meters of cell center.

f) Sol_1000: Mean solar radiation value for all cells with centers ≤ 1000 meters of cell center.

Surface Area Ratio:

The surface area ratio is defined as the true surface area within each cell divided by the planimetric area of that cell. We created a technique to calculate the true surface area of each cell based on the elevation of that cell plus the elevation of the 8 surrounding cells. Detailed explanations of this technique and an analysis of it's accuracy are available on-line (Jenness 2001). We divided the surface area of each cell by the planimetric area of each cell to get the surface ratio.

We then generated neighborhood grids where each cell value represented the mean surface area ratio value for all those cells whose cell centers lay within the specified distance.

Surface Ratio Grids (Datasets included on CD 4):

a) Ratio_1: Surface Area Ratio value on the cell

b) Ratio_100: Mean Surface Area Ratio value for all cells with centers $\leq$ 100 meters of cell center.

c) Ratio_200: Mean Surface Area Ratio value for all cells with centers $\leq$ 200 meters of cell center.

d) Ratio_400: Mean Surface Area Ratio value for all cells with centers $\leq$ 400 meters of cell center.

e) Ratio_800: Mean Surface Area Ratio value for all cells with centers $\leq$ 800 meters of cell center.

f) Ratio_1000: Mean Surface Area Ratio value for all cells with centers $\leq$ 1000 meters of cell center.

Road Density:

Road density values reflect the proportion of cells in a neighborhood that have roads on them. A value of 0 means there are no roads in the neighborhood while a value of 1 indicates that every cell in the neighborhood has a road. Road locations were derived from 1992 TIGER (Topologically Integrated Geographic Encoding and Referencing) files provided by the US Census Bureau, which provide the best road coverage for remote areas that we have found. We used all roads in this dataset, ranging from interstates to vehicular trails.

We then generated neighborhood grids where each cell value represented the mean road density value for all those cells whose cell centers lay within the specified distance.

Road Density Grids (Datasets included on CD 5):

a) Road_1: Either 1 or 0, depending on whether the cell contains a road.

b) Road_100: Proportion of cells with roads for all cells with centers ≤ 100 meters of cell center.

c) Road_200: Proportion of cells with roads for all cells with centers ≤ 200 meters of cell center.

d) Road_400: Proportion of cells with roads for all cells with centers ≤ 400 meters of cell center.

e) Road_800: Proportion of cells with roads for all cells with centers ≤ 800 meters of cell center.

f) Road_1000: Proportion of cells with roads for all cells with centers ≤ 1000 meters of cell center.

Protection:

This idea is adapted from Terry Johnson's idea of Local Curvature (Johnson 1996), in which nearby topographic features such as cliffs or hills can be considered to provide protection from wind. The amount of protection provided by these features depends on two factors: *Height* and *Proximity*. The protection that a feature offers increases with both closeness and height.

We originally tried using Johnson's actual algorithm, defined as the "maximum inverse radius of curvature of a circular arc from each point to elevations along a ray, centered above the point in question." (Johnson 1996). After some trial and error we determined that there were problems with the output under certain conditions, so we derived another method would try to capture the concept of protection but without using the maximum inverse radius of curvature method to calculate it.

The method we adopted was to take the two factors we were interested in, height and proximity, and combine them in a such a way that both factors would influence the final cell value. We did this by measuring the angle from each cell to cells within 2,000 meters, in eight directions, and then dividing that angle by the horizontal distance to the cells (Figures 3 and 4). We then took the maximum value from each of the eight directions and averaged them, and the final product was a grid in which the value of each cell in the grid reflected the average of the maximum protection values calculated within 2,000 meters in eight directions from that cell.

It may be debatable as to whether the protection offered by some topographic feature can be quantified this easily, but this method does have the advantage of producing protection values proportional to the height and proximity of a feature. In other words, the protection value of a 100-meter cliff will be twice that of a 50-meter cliff, assuming the cliffs are both the same distance away. Likewise, the protection value of a cliff 50 meters away will be twice that of a cliff 100 meters away, assuming both cliffs are the same height.

We then generated neighborhood grids where each cell value represented the mean protection value for all those cells whose cell centers lay within the specified distance.

Protection Grids (Datasets included on CD 6):

a) Prot_1: Protection value on the cell

b) Prot_100: Mean Protection value for all cells with centers $\leq$ 100 meters of cell center.

c) Prot_200: Mean Protection value for all cells with centers $\leq$ 200 meters of cell center.

d) Prot_400: Mean Protection value for all cells with centers $\leq$ 400 meters of cell center.

e) Prot_800: Mean Protection value for all cells with centers $\leq$ 800 meters of cell center.

f) Prot_1000: Mean Protection value for all cells with centers $\leq$ 1000 meters of cell center.

Methods

Using our 355 owl locations, we developed lists of 355 analytic data layer values for each of our 36 analytic data layers (i.e. 355 *Slope_1* values, 355 *Prot_200* values, etc.). Based on these lists we determined 100 percentile ranges, centered about the median, within the full range of values for each analytic variable (i.e. for *Slope_1* we determined the minimum and maximum *Slope_1* values that would correspond with the middle 100%, 99%, 98% … 1% of the owl locations). We examined each analytic variable in terms of the proportion of the landscape that corresponded with each percentile range, with the assumption that lower landscape proportions at particular percentile levels represented more selective use of the landscape, and thus analytic data layers with relatively low landscape proportion values would be

relatively more important to owls. For example, given a constant percentile level (say the middle 90% of owl locations), if the range of values in an analytic data layer encompassed 90% of the owl locations and yet only included 20% of the landscape, then that layer would likely be relatively more important than a data layer that required, 70% of the landscape to encompass these same owl locations. Owls would be concentrating themselves more into the first data layer and therefore that first data layer would likely be more important to them. In all further discussion, the term "percentile level" refers to the central X% of analytic data layer values taken from our 355 owl locations.

We then developed a series of multi-variable models based on these individual analyses. We looked at all individual analytic data layer analyses in which the range of the data layer values included $\geq$ 90% of the owl locations, and identified which of the various scales of each general variable type was most selective at each percentile level between 90% and 100%. For example, just looking at the 6 spatial scale variables of the *Slope* variable type, we identified which *Slope* spatial scale variable appeared to be most important at the 90th percentile level, then which *Slope* spatial scale appeared most important at the 91st percentile level, etc. Finally, we developed a series of landscape models reflecting various combinations of our best analytic data layers to see which combination produced the best (i.e. lowest) landscape proportions at different owl predictive accuracy levels.

Results

Individual Analyses: We generated 100 new grids for each of our 36 analytic data layers, where each new grid represented the landscape that lay within the 1st, 2nd, ... 100th percentile of the range of owl location data. We then plotted the proportion of landscape that fell within the range for each percentile and for each analytic data layer (Figures 5-10). Based on these individual analyses, we determined that the *Road Density* data layers could be discarded because the proportion of owls that were classified correctly never deviated very far from the proportion of the landscape predicted, inferring that the presence of roads (at least in terms of how we defined them) did not appear to have a strong influence over the owls' locations

(Figure 9). We also discarded the *Solar Radiation* layers (Figure 7) because at the higher percentile levels the landscape proportions stayed relatively high as the proportion of owls decreased, inferring that the changes in the proportion of owls was due to something other than solar radiation values.

This left us with four general analytic data types (*Elevation, Slope, Protection* and *Surface Ratio*), each represented at 6 spatial scales. For each general data type and for each percentile level between 0.9 and 1.0, we identified the spatial scale that produced the lowest proportion of the landscape while still encompassing that particular percentage of owl locations. For example, given, say, the middle 90% of slope values derived from our 355 owl locations for each of our 6 spatial scales, we find that the corresponding ranges of data for each spatial scale produce the landscape proportions in Table 2.

The important point to gain from Table 2 is that, at the 90th percentile, the Slope variable at the 400m spatial scale level had the lowest proportion of landscape. Therefore, for Slope at the 90th percentile, hereafter we only consider the 400m spatial scale for future models. We use this same process to identify the most significant spatial scale for Elevation, Protection and Surface Ratio at the 90th percentile, then again for all variables at the 91st percentile on up to the 100th percentile (Table 3). We did this for all variables in which the actual proportion of owl locations within the range of values was $\geq$ 90%. Two variables (Elev_1 and Ratio_1) actually contained $\geq$ 90% of the owl locations when using the 89th percentile ranges so we also included those variables in further analyses.

This gave us the best spatial scale grid for each data class (Slope, Elevation, Protection and Surface Ratio) for all percentile levels, after considering all grids containing $\geq$ 90% of the owl locations. This resulted in 12 Elevation grids, 12 Surface Ratio grids, 11 Protection grids and 11 Slope grids (these 46 datasets are provided in ArcInfo GRID format on CD 7). We then examined combinations of these grids in which each combination included one grid from each data class. This led to 17,424 combinations ($12\times12\times11\times11$), each of which produced a grid representing those areas which met all four ranges of data. We then tested each of these combination grids to see what proportion of owl locations was correctly classified.

As with the individual comparisons, we decided that the best combinations would be those that correctly classified the greatest number of owl locations while predicting the lowest proportion of the landscape. We plotted the proportion of owl locations correctly classified against the proportion of the landscape predicted to be owl habitat, then identified which combination produced the lowest proportion of the landscape at each percentage level of owl location prediction accuracy.

Owl predictive accuracies ranged from 76% to 100% and the lowest landscape proportion values ranged from 27% (when 77% of owl locations were predicted correctly) to 81% (when 100% of owl locations were predicted correctly) (Table 4). These 25 combination model datasets are provided in ArcInfo GRID format on CD 7.

Discussion:

Of our six general data types, only slope, elevation, protection and surface ratio appeared to contribute meaningful information to our habitat models. Surprisingly, the average annual solar radiation appeared to have little relationship with where owls were located. As illustrated in Figure 7, solar radiation at all spatial scales showed an interesting trend at the upper percentiles of owl location values in which each change in owl location percentile corresponded with very little change in the total proportion of the landscape. For example, at the 1000m scale, the range of values derived from 100% of the owl locations corresponded to 99.9% of the landscape, while the range of values from only 65% of the owl locations still corresponded to 90% of the landscape. Therefore excluding the extreme 35% of owl locations only reduced the proportion of landscape by 10%, suggesting that the central 65% of owl location values still represent nearly the full range of solar radiation values on the landscape. Whatever qualities lead an owl to occupy a particular place on the landscape does not appear to be related to the solar radiation on the landscape.

Road density also did not appear to play an important role in determining where owls were located. As illustrated in Figure 9, the proportions of the landscape that fell within road density percentile levels were almost identical to the actual percentile levels, implying that the percentage of owl locations

accurately predicted by the model was due more to the simple proportion of the landscape classified as "True" rather than the actual road density on any particular area. However, analysis of road density percentile levels was problematic because of the high number of "0" values at all spatial scales. Even at the 1000m scale, which showed the most variation in road density, there were 183 (51.5%) cases with 0% road density, meaning that all percentile ranges had a lower road density value of 0% (Figure 11).

Our set of multi-variable habitat models are therefore derived from 6 spatial scales each of Slope, Elevation, Protection and Surface Ratio values. The series of models show progressively greater predictive accuracy levels, based on the data we used to derive them, ranging from 76% predictive accuracy up to 100% (Figure 12, Table 4).

We do not rank these models based solely upon the predictive accuracy, however. Even though a model predicts 100% of our owl locations correctly, the fact that such a model also predicts 80% of the landscape as owl habitat will likely render it useless to most land managers. Therefore we offer the entire series of "best" models so that land managers can consider the implications of different levels of predictive accuracy. For example, a person might consider dropping from 100% down to 95% and find that now they only have to worry about 42% of the landscape (Table 4). Dropping to 90% reduces the proportion of the landscape to 34%, and the lowest landscape proportion achieved by our models was 27% with a corresponding owl predictive accuracy level of 77% (Figure 13).

There were no clear patterns among our 25 best models, although it is interesting that the models for the 95% - 100% predictive accuracy levels all used the 1000m scale level for all four variables (Table 4). Nineteen of the 25 models used Elevation at the 1000m scale, suggesting that the average elevation within a kilometer from an owl may be relatively more important than the average elevation within smaller distances, however Figure 5 suggests that there are only marginal differences between the landscape proportions at each percentile level among Elevation spatial scales.

In sum, these 25 models show the arrangements of our 4 variables at 6 spatial scales which predict the minimum proportion of landscape at 25 progressively increasing accuracy levels. We leave it to managers to decide which predictive accuracy level makes the most sense for their particular project.

Suggestions for Further Research

Incorporate Vegetation Data: The single greatest weakness of our set of models was a lack of vegetation data. Future models would likely be far more useful if data on certain habitat types with well-known spotted owl associations could be included, such as mixed-conifer forest types and pine/oak mixes, and avoidance of pure pine stands. Our models, because they were based solely on topographic data, likely include large areas of grassland and pinyon/pine forests which are unlikely places to find spotted owls.

Solar Radiation at season of survey: Solar radiation did not come out as a significant variable, which was somewhat of a surprise. However, our solar radiation values reflected the annual amount of radiation hitting an area while we only surveyed during the summer season. It is possible that a solar radiation index based only on the summer season, especially if modified by average daily cloud cover, might show more significance.

Landscape morphometry; ravines vs. plateaus vs. slopes: Spotted owls are known to prefer generally steep slopes and are often found within incised ravines on hillsides. It may be useful to identify these features on the landscape.

Finer-scale data. In all variables that we considered, and in other potential variables, we would likely benefit by using finer-scale data. At the time of this study the only available elevation dataset that covered our entire study area contained elevation values approximately 92 meters apart. Such coarse data make it impossible to identify many landscape features that may be important to spotted owls. Johnson (1996, 1998) found that topographic models derived from 30m data did much better at identifying topographic features important to spotted owls than similar models derived from 92m data, especially when the 30m data had not been smoothed. This higher-resolution data has recently become available for the entire study

area from the National Elevation Dataset (Gesch et al. 2002) and will soon be available from the 2000 Shuttle Radar Topography Mission (JPL 2000).

Check accuracy of models on a separate dataset (i.e. Forest Service spotted owl data): The models presented in this report have been developed and tested on a single dataset of owl locations and therefore their true predictive accuracy is unknown. These models should be tested on separate owl location datasets to see how well they do.

Reclass Road Densities: Our measures of road densities may have been adversely affected by the high proportion of 0%-density areas. It may make more sense to reclassify the density values into presence vs. absence of roads.

Acknowledgments

We would like to thank Terry Johnson for his help and advice during early stages of this project, and Bill Huber for some valuable ArcView tools he provided free of charge from his website (Quantitative Decisions 1999). We would also like to thank the USFS Rocky Mountain Forest and Range Experiment Station for funding this project.

References:

Cully, J. and W. Austin. 1993. Endangered and threatened wildlife and plants: final rule to list the Mexican spotted owl as a threatened species. Fed. Register 58:14248-14271

ESRI. 2000a. ArcView GIS 3.2a. Redlands, CA, USA: Environmental Systems Research Institute, Inc.

ESRI. 2000b. ArcView spatial analyst. [ArcView 3.x Extension]. Version 2. Redlands, CA, USA: Environmental Systems Research Institute, Inc.

Ganey, J.L. and J.A. Dick. 1995. Habitat relationships of Mexican spotted owls: current knowledge. Chapter 4:1-42 *in*: W.M. Block, F. Clemente, J.F. Cully, J.L. Dick Jr., A.B. Franklin, J.L. Ganey, F.P. Howe, W.H. Moir, S.L. Spangle, S.E. Rinkevich, D.L. Urban, R. Vahle, J.P. Ward Jr. and G.C. White. Recovery plan for the Mexican spotted owl. Albuquerque, NM.

Ganey, J.L., G.C. White, A.B. Franklin and J.P. Ward, Jr. 1999a. Monitoring population trends of Mexican spotted owls in Arizona and New Mexico: A pilot study. Study plan no. RM-4251-6-1. Rocky Mountain Research Station, Flagstaff, AZ.

Ganey, J.L., S. Ackers, P. Fonken, J. Jenness, K. Kessler, K. Nodal, P. Shaklee, and E. Swarthout. 1999b. A pilot study on monitoring populations of Mexican spotted owls in Arizona and New Mexico: progress report. USDA Forest Service, Rocky Mountain Research Station 2500 South Pine Knoll Drive, Flagstaff, AZ 86001. Available at http://www.rmrs.nau.edu/lab/4251/spowmonitoring.html

Gesch D, Oimoen M, Greenlee S, Nelson C, Steuck M, Tyler D. 2002. The national elevation dataset. Photogrammetric Engineering & Remote Sensing 68(1):5-11.

Grubb, T.G., J.L. Ganey and S.R. Masek. 1997. Canopy closure around nest sites of Mexican spotted owls in northcentral Arizona. Journal of Wildlife Management 61(2):336-342

Jenness, J. 2001a. Surface areas and ratios from elevation grid. [ArcView 3.x Extension] Flagstaff, AZ, USA: Jenness Enterprises. Available at http://www.jennessent.com/arcview/surface_areas.htm.

Johnson, T.H. 1996. Topographic model of potential spotted owl habitat in northern New Mexico. Santa

Fe National Forest PO 43-8379-5-0391. Los Alamos National Laboratory Agreement C-5379. P.O. Box 327, Los Alamos, NM 87544. 10 pp.

Johnson, T.H. 1998. Topographic-Landsat model of suitable spotted owl habitat around Los Alamos national laboratory. Los Alamos National Laboratory Agreement C-6832. P.O. Box 327, Los Alamos, NM 87544. 9 pp.

JPL. 2002 Sep. Shuttle Topography Radar Mission [Web Page]. Located at: http://www.jpl.nasa.gov/srtm. Accessed 2002 Sep.

Peery, M.Z., R.J. Gutierrez and M.E. Seamans. 1999. Habitat composition and configuration around Mexican spotted owl nest and roost sites in the Tularosa mountains, New Mexico. Journal of Wildlife Management 63(1):36-43

Quantitative Decisions. 1999. Reproject Grids [ArcView 3.x extension]: Quantitative Decisions. Available at: http://arcscripts.esri.com/details.asp?dbid=11368

Rinkevich, S.E., J.L. Ganey, W.H. Moir, F.P. Howe, F. Clemente, and J.F. Martinez-Montoya. 1995. Recovery Units Pp. 36-51 *in:* W.M. Block, F. Clemente, J.F. Cully, J.L. Dick Jr., A.B. Franklin, J.L. Ganey, F.P. Howe, W.H. Moir, S.L. Spangle, S.E. Rinkevich, D.L. Urban, R. Vahle, J.P. Ward Jr. and G.C. White. Recovery plan for the Mexican spotted owl. Albuquerque, NM.

U.S. Naval Observatory, 2000. Calculator for altitude and azimuth of the sun or moon during one day, located in "Data Services" in the U.S. Naval Observatory Applications Department. Web Address: <http://aa.usno.navy.mil/AA/>

Ward, J.P., Jr., A.B. Franklin, S.E. Rinkevich, and F. Clemente. 1995. Distribution and abundance of Mexican spotted owls. Chapter 1:(1-14) *in*: W.M. Block, F. Clemente, J.F. Cully, J.L. Dick Jr., A.B. Franklin, J.L. Ganey, F.P. Howe, W.H. Moir, S.L. Spangle, S.E. Rinkevich, D.L. Urban, R. Vahle, J.P. Ward Jr. and G.C. White. Recovery plan for the Mexican spotted owl. Albuquerque, NM.

Tables:

Table 1: Number of grid cells corresponding to neighborhood sizes

Neighborhood Size	Number of Grid Cells
1m	1
100m	5
200m	13
400m	49
800m	197
1000m	317

Table 2: Proportion of landscape corresponding to all spatial scales of slope values at 90th percentile

Percentile Level	Spatial Scale	Range of Data Values	Proportion of Landscape	Actual Proportion of Owls Within Range
90%	1m	0.39° - 27.79°	79%	91.5%
90%	100m	1.65° - 26.46°	65%	91.5%
90%	200m	2.12° - 23.64°	62%	89.9%
90%	400m	2.84° - 21.83°	60%	90.7%
90%	800m	2.99° - 21.16°	62%	89.9%
90%	1000m	2.87° - 20.71°	64%	90.1%

Table 3: Landscape proportions and owl location proportions of individual grid analyses, showing only those spatial scales with the lowest landscape proportion at each percentile level

Percentile Level	Data Type And Best Spatial Scale	Range of Data Values	Proportion of Landscape	Actual Proportion of Owls Within Range
89%	Elev_1	1951.0000 - 2804.0000	61.91%	90.42%
	Ratio_1	100023.2813 - 113180.8984	73.36%	90.14%
90%	Elev_1	1951.0000 - 2804.0000	61.91%	90.42%
	Prot_200	0.0088 - 0.0842	57.70%	90.42%
	Ratio_800	100691.5078 - 110968.3047	51.06%	90.14%
	Slop_400	2.8426 - 21.8324	59.88%	90.70%
91%	Elev_400	1954.2449 - 2811.3264	62.29%	91.83%
	Prot_200	0.0088 - 0.0845	57.72%	90.99%
	Ratio_200	100237.5313 - 113330.3984	55.26%	92.11%
	Slop_400	2.7408 - 21.8324	60.76%	91.83%
92%	Elev_200	1951.3846 - 2821.2692	62.36%	92.11%
	Prot_800	0.0108 - 0.0738	60.37%	91.55%
	Ratio_400	100326.6875 - 112088.3359	56.80%	92.39%
	Slop_400	2.7408 - 21.9885	60.82%	92.39%
93%	Elev_400	1949.2347 - 2823.0613	63.57%	92.96%
	Prot_200	0.0077 - 0.0887	61.02%	92.96%
	Ratio_400	100325.4727 - 112224.4258	56.90%	92.96%
	Slop_400	2.4406 - 22.4563	63.73%	92.68%
94%	Elev_200	1945.0769 - 2836.8462	64.12%	94.65%
	Prot_800	0.0103 - 0.0760	61.98%	93.80%
	Ratio_800	100418.5156 - 112073.8750	59.59%	94.08%
	Slop_800	2.5731 - 22.2386	67.69%	94.37%
95%	Elev_1000	1931.8959 - 2859.9399	66.16%	95.49%
	Prot_400	0.0087 - 0.0825	62.98%	95.21%
	Ratio_1000	100363.7266 - 111710.0469	63.61%	95.21%
	Slop_400	2.0099 - 22.8415	68.21%	95.21%
96%	Elev_1000	1931.8959 - 2866.0663	66.20%	95.77%
	Prot_1000	0.0086 - 0.0763	68.41%	95.77%
	Ratio_400	100181.2969 - 112309.1797	64.00%	96.06%
	Slop_400	1.9095 - 23.0251	69.37%	95.49%
97%	Elev_1000	1929.3234 - 2868.5173	66.44%	96.90%
	Prot_800	0.0075 - 0.0784	71.67%	96.62%
	Ratio_1000	100333.6641 - 113195.0469	65.15%	97.18%
	Slop_800	2.0809 - 23.4302	73.52%	96.62%
98%	Elev_1000	1929.0474 - 2873.1418	66.49%	98.31%
	Prot_800	0.0072 - 0.0795	72.94%	97.75%

	Ratio_1000	100333.6641 - 113647.0547	65.19%	97.75%
	Slop_1000	2.0986 - 23.2058	74.82%	97.75%
	Elev_1	1431.0000 - 2905.0000	93.22%	98.87%
99%	Prot_1000	0.0066 - 0.0795	76.37%	99.44%
	Ratio_1000	100200.8281 - 113727.8828	72.34%	99.44%
	Slop_1000	1.6609 - 23.3774	80.51%	98.87%
	Elev_1000	1328.4291 - 3014.1072	96.05%	100.00%
100%	Prot_1000	0.0036 - 0.0795	88.16%	100.00%
	Ratio_1000	100066.6172 - 113727.8828	85.34%	100.00%
	Slop_1000	1.0066 - 24.4591	89.06%	100.00%

Table 4: Best models at each Predictive Accuracy Percentile Level, from all possible permutations of best individual grids (see Table 3).

Percent of Owl Locations Accurately Predicted	Proportion Landscape Predicted as Owl Habitat	Slope		Elevation		Ratio		Protection		Record Number
		Scale	Inner Percentile Range	Scale	Inner Percentile Range	Scale	Inner Percentile Range	Scale	Inner Percentile Range	
0.76	0.324407	Slop_400	0.9	Elev_1	0.89	ratio_1	0.89	Prot_200	0.9	[rec 0]
0.77	0.266708	Slop_400	0.9	Elev_1	0.89	Ratio_800	0.9	Prot_200	0.9	[rec 11]
0.78	0.268624	Slop_400	0.92	Elev_400	0.91	Ratio_800	0.9	Prot_200	0.9	[rec 3443]
0.79	0.270388	Slop_400	0.96	Elev_400	0.91	Ratio_800	0.9	Prot_200	0.9	[rec 9779]
0.80	0.272557	Slop_400	0.9	Elev_200	0.94	Ratio_800	0.9	Prot_200	0.9	[rec 671]
0.81	0.274705	Slop_400	0.95	Elev_200	0.94	Ratio_800	0.9	Prot_200	0.9	[rec 8591]
0.82	0.279627	Slop_400	0.92	Elev_1000	0.95	Ratio_800	0.9	Prot_200	0.9	[rec 3971]
0.83	0.280735	Slop_400	0.9	Elev_1000	0.98	Ratio_800	0.9	Prot_200	0.9	[rec 1199]
0.84	0.281236	Slop_400	0.92	Elev_1000	0.98	Ratio_800	0.9	Prot_200	0.9	[rec 4367]
0.85	0.283119	Slop_400	0.96	Elev_1000	0.98	Ratio_800	0.9	Prot_200	0.9	[rec 10703]
0.86	0.289277	Slop_400	0.96	Elev_1000	0.98	Ratio_800	0.9	Prot_200	0.93	[rec 10706]
0.87	0.307917	Slop_400	0.95	Elev_1000	0.98	Ratio_800	0.9	Prot_400	0.95	[rec 9124]
0.88	0.311134	Slop_800	0.94	Elev_1000	0.98	Ratio_800	0.9	Prot_400	0.95	[rec 7540]
0.89	0.327575	Slop_800	0.94	Elev_1000	0.98	Ratio_800	0.94	Prot_200	0.93	[rec 7582]
0.90	0.341841	Slop_400	0.95	Elev_1000	0.98	Ratio_1000	0.97	Prot_200	0.93	[rec 9199]
0.91	0.344984	Slop_1000	1	Elev_1000	0.98	Ratio_1000	0.97	Prot_200	0.93	[rec 17119]
0.92	0.367476	Slop_800	0.94	Elev_1000	0.98	Ratio_1000	0.98	Prot_400	0.95	[rec 7628]
0.93	0.392488	Slop_1000	0.99	Elev_1000	0.98	Ratio_1000	0.99	Prot_400	0.95	[rec 15559]
0.94	0.392768	Slop_1000	1	Elev_1000	0.98	Ratio_1000	0.99	Prot_400	0.95	[rec 17143]
0.95	0.424754	Slop_1000	0.99	Elev_1000	0.98	Ratio_1000	0.97	Prot_1000	0.99	[rec 15541]
0.96	0.425151	Slop_1000	1	Elev_1000	0.98	Ratio_1000	0.98	Prot_1000	0.99	[rec 17136]
0.97	0.469202	Slop_1000	0.99	Elev_1000	0.98	Ratio_1000	0.99	Prot_1000	0.99	[rec 15563]
0.98	0.477137	Slop_1000	1	Elev_1000	0.98	Ratio_1000	0.99	Prot_1000	1	[rec 17148]
0.99	0.686472	Slop_1000	0.99	Elev_1000	1	Ratio_1000	0.99	Prot_1000	0.99	[rec 15827]
1.00	0.805501	Slop_1000	1	Elev_1000	1	Ratio_1000	1	Prot_1000	1	[rec 17423]

Figures:

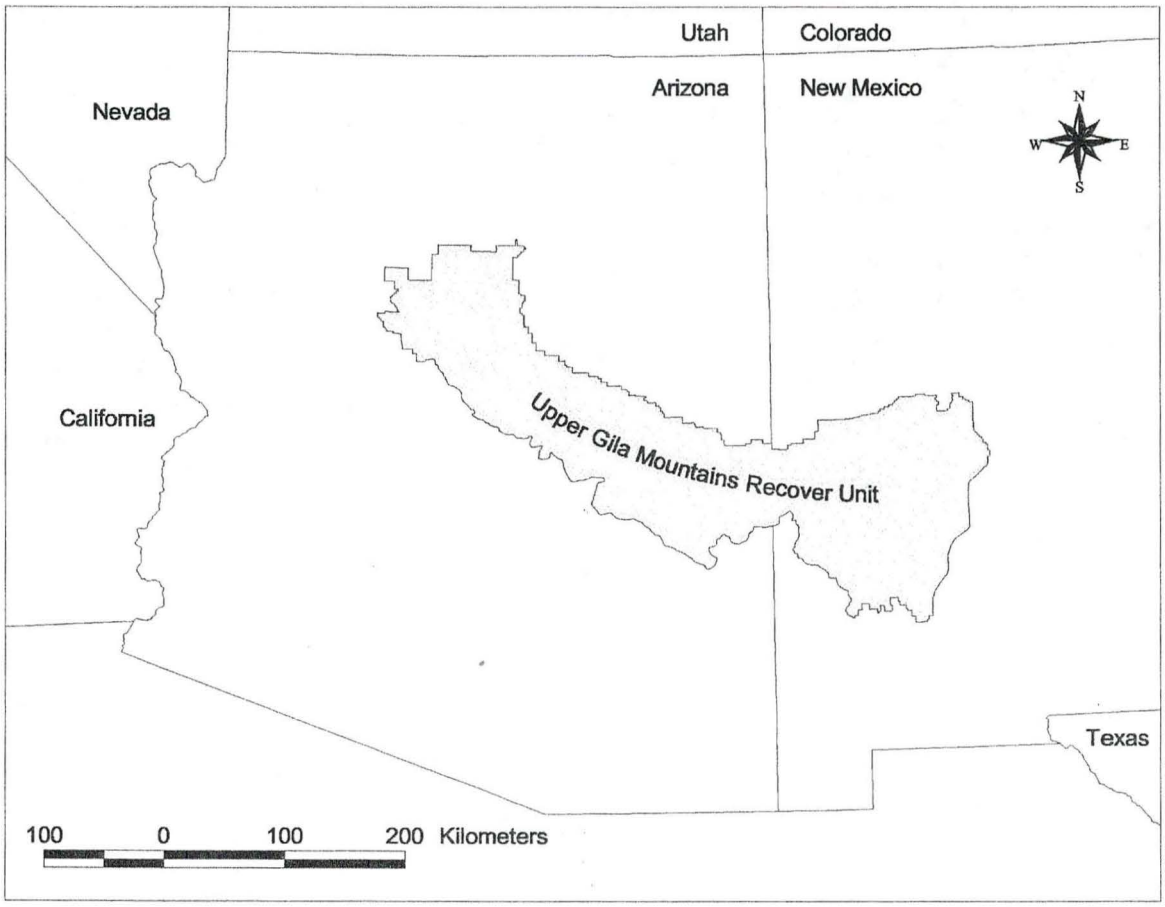

Figure 1: We used the Upper Gila Mountains recovery unit for our study area. Our owl locations were taken from randomly-distributed watersheds within this area, and our landscape variables and predictive models encompass the entire area.

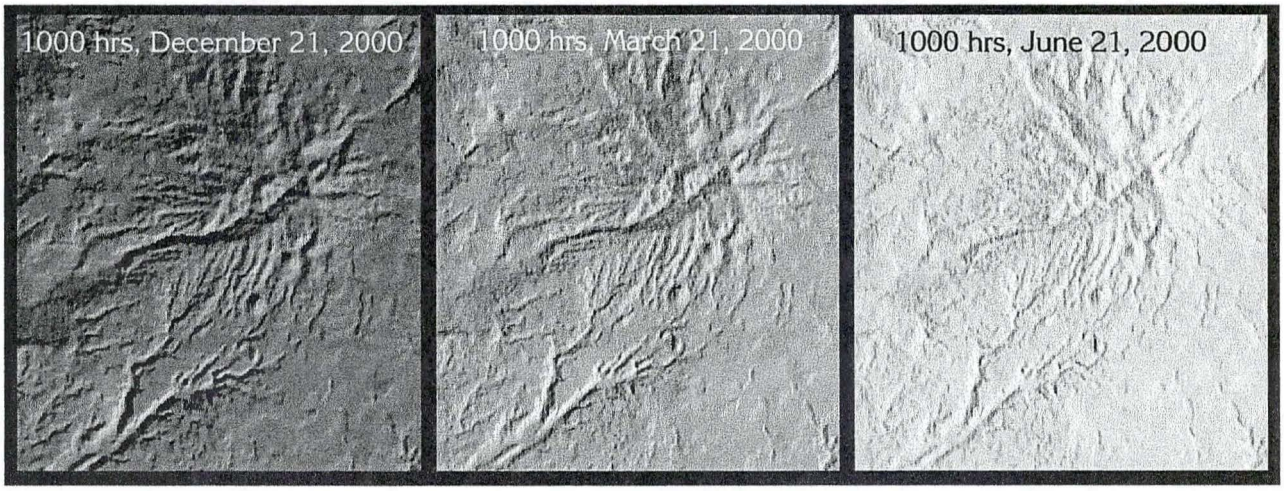

Figure 2: Solar radiation grids for 10:00 am on three days in the year 2000, shaded from black (cell value = 0), meaning no sunlight hit that cell) to white (cell value = 255, meaning that cell faced the sun directly). We calculated these grids for all hours of the day in which the sun was up on that day, and added them to get daily totals for each of the 12 days of the year. We then added these 12 daily totals and divided the sum by 12 to get a solar radiation grid representing the average amount of daily radiation each cell gets over the entire year.

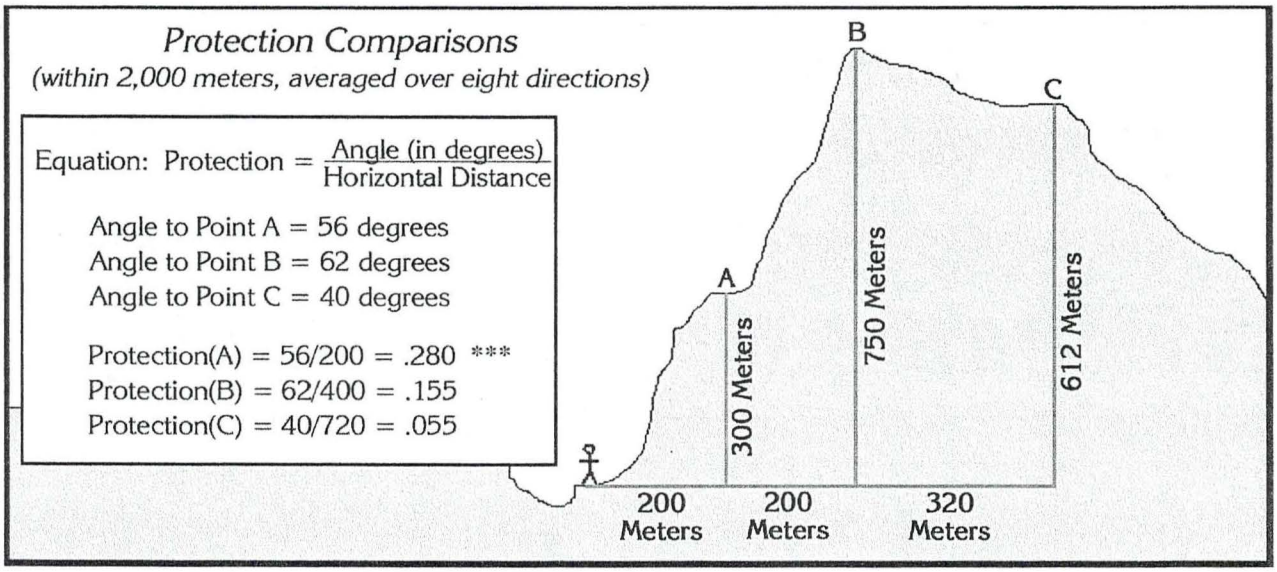

Figure 3: Protection depends on both proximity and height. In this case, Point B is both higher and at a steeper angle from the origin than Point A, yet Point A outscores Point B because it is closer. Using this method, we would conclude that a 300-meter cliff located 200 meters away would offer almost twice as much protection as a 750-meter cliff located 400 meters away (with respective scores of 0.280 and 0.155). This calculation is repeated eight times in eight directions, and the final cell value reflects the average of maximum protection values calculated in the eight directions.

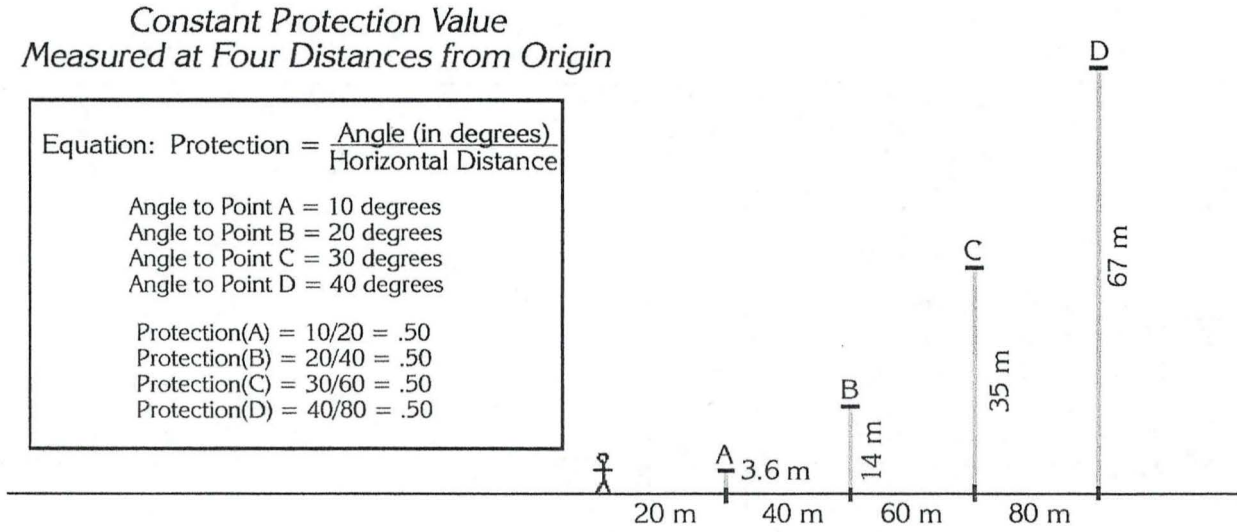

Figure 4: Different combinations of height and proximity can produce the same protection values. In this example, a 67-meter cliff 80 meters away offers the same protection value as a 3.6-meter cliff 20 meters away.

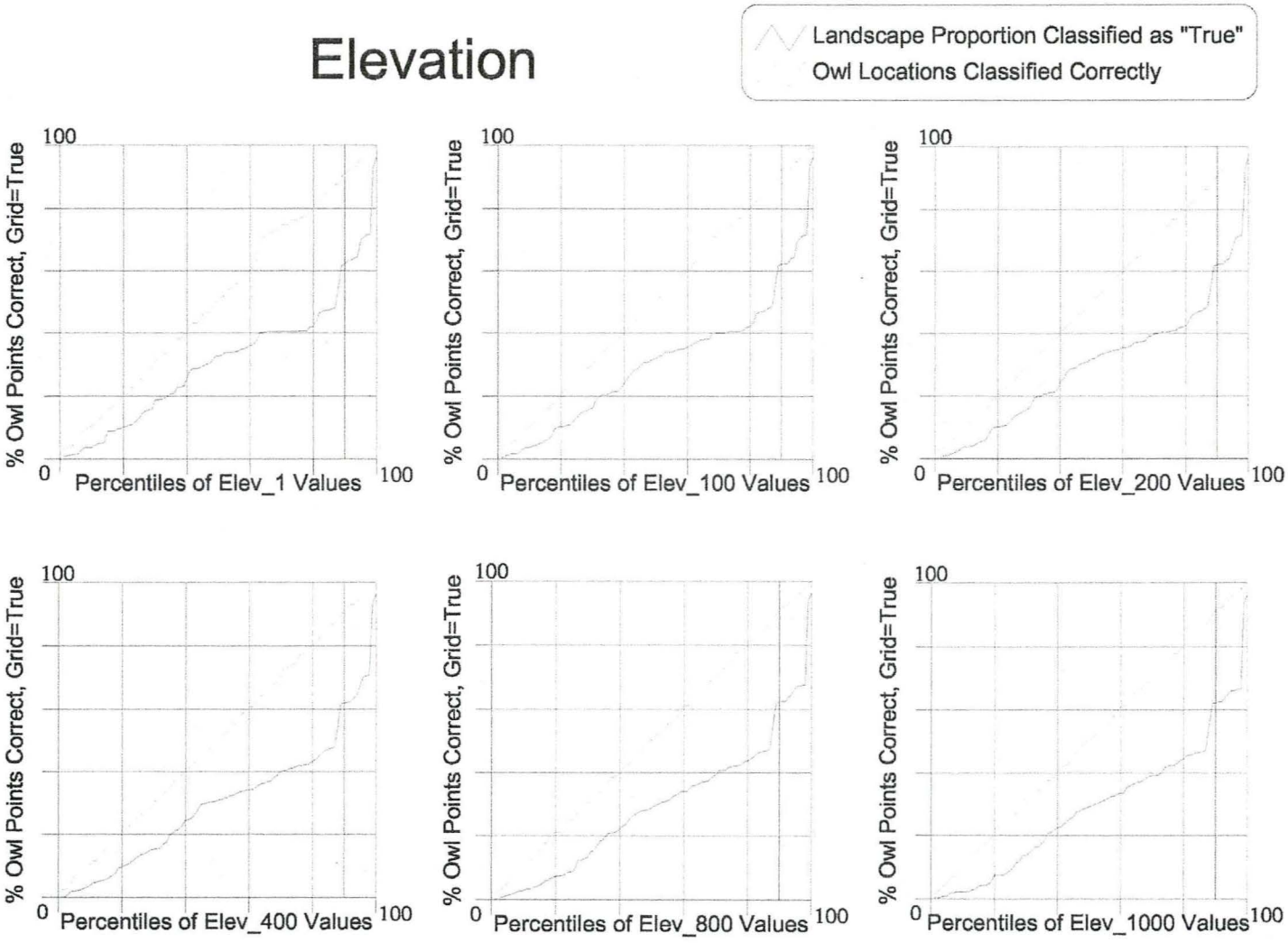

Figure 5: Proportions of the landscape corresponding with percentile ranges of Elevation values, at 6 spatial scales.

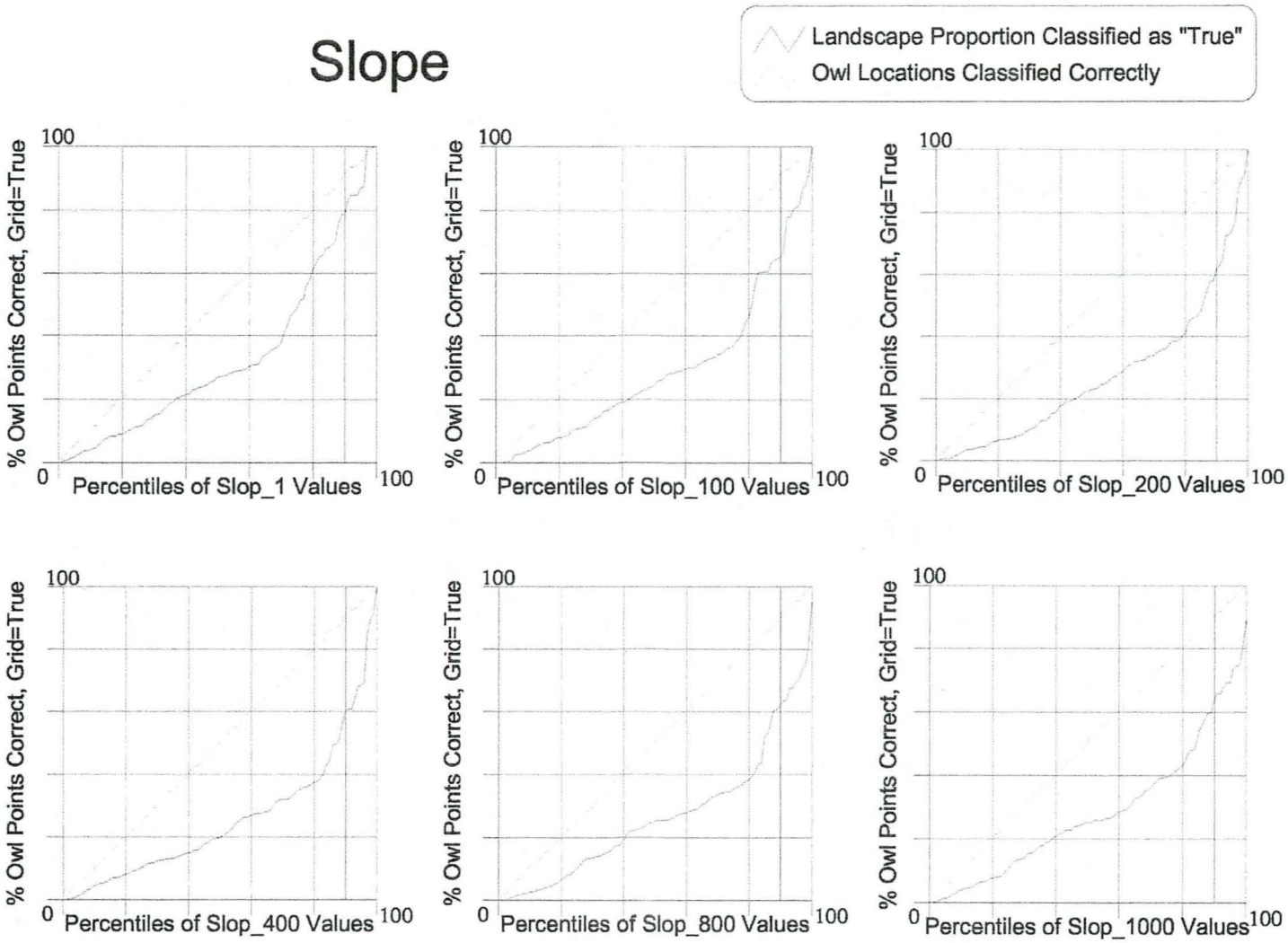

Figure 6: Proportions of the landscape corresponding with percentile ranges of Slope values, at 6 spatial scales.

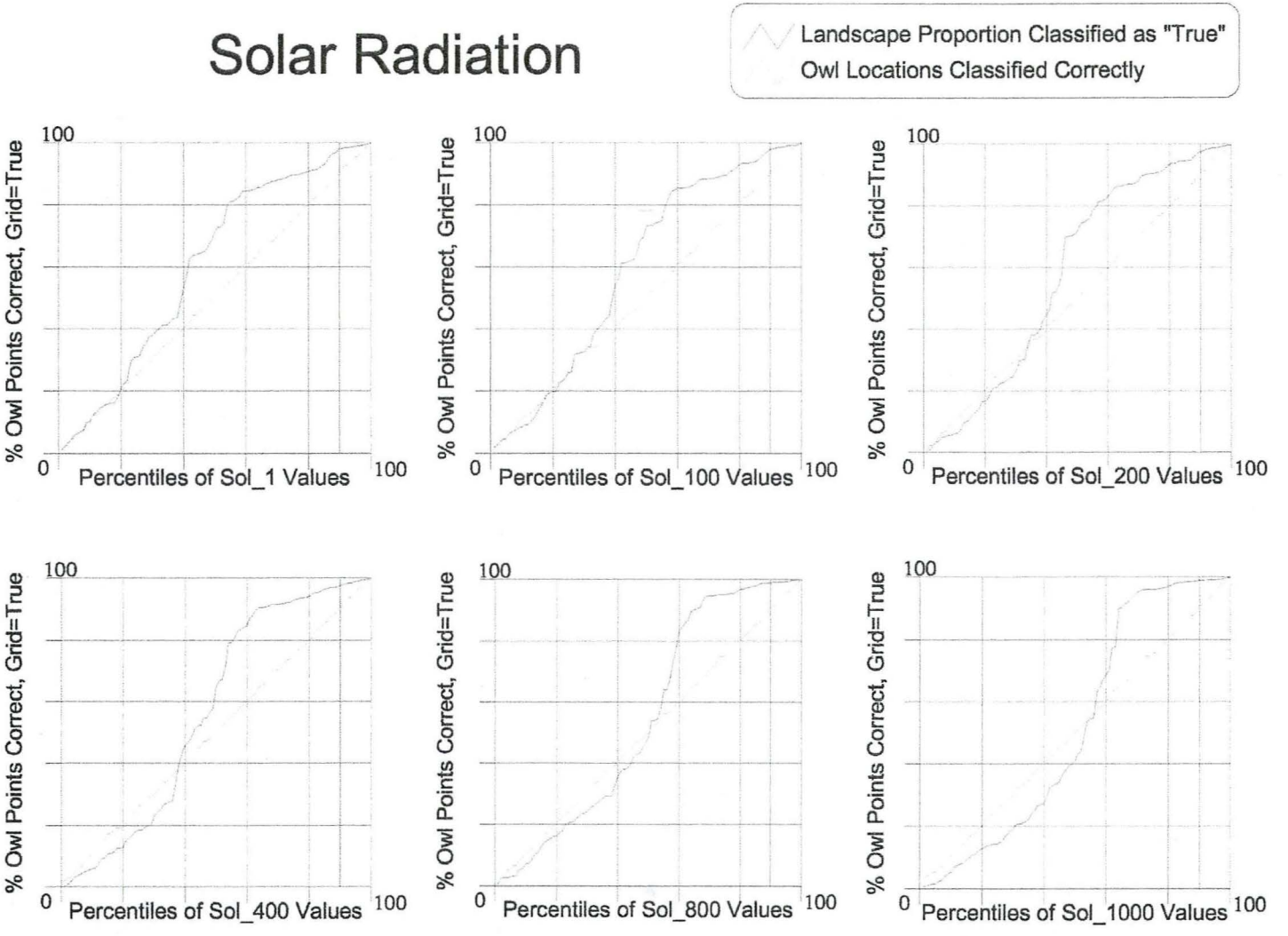

Figure 7: Proportions of the landscape corresponding with percentile ranges of Solar Radiation values, at 6 spatial scales.

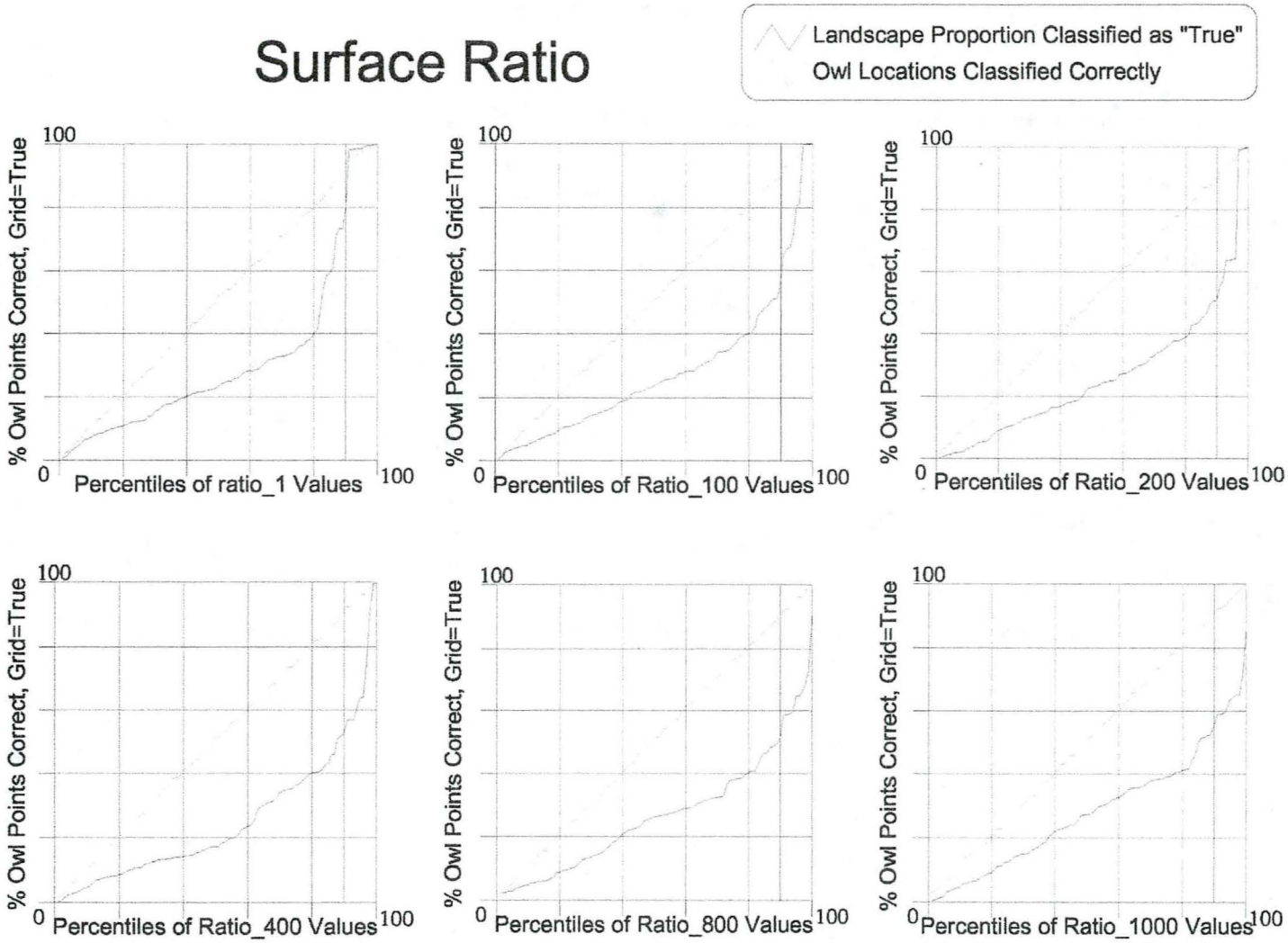

Figure 8: Proportions of the landscape corresponding with percentile ranges of Surface Ratio values, at 6 spatial scales.

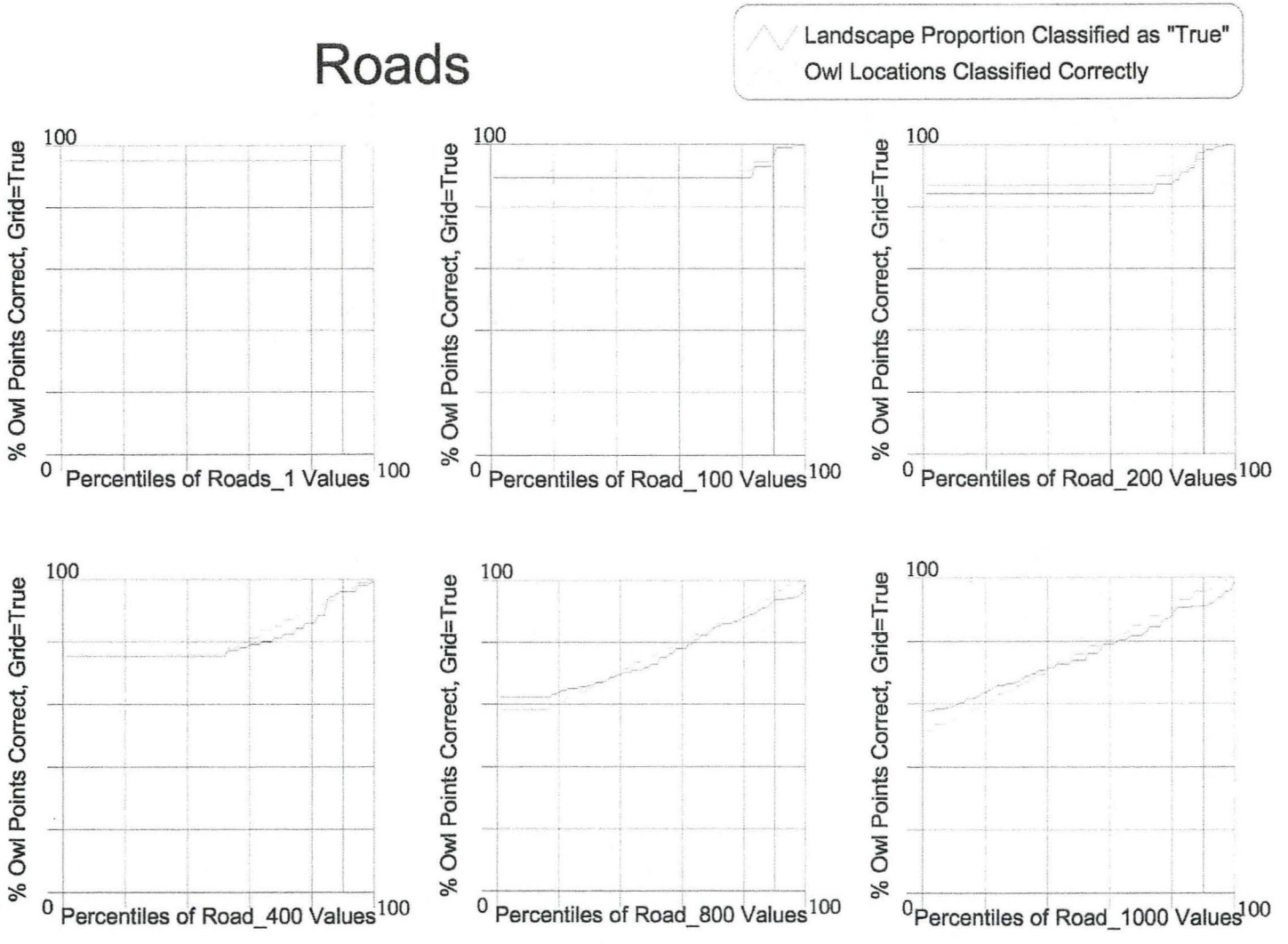

Figure 9: Proportions of the landscape corresponding with percentile ranges of Road Density values, at 6 spatial scales.

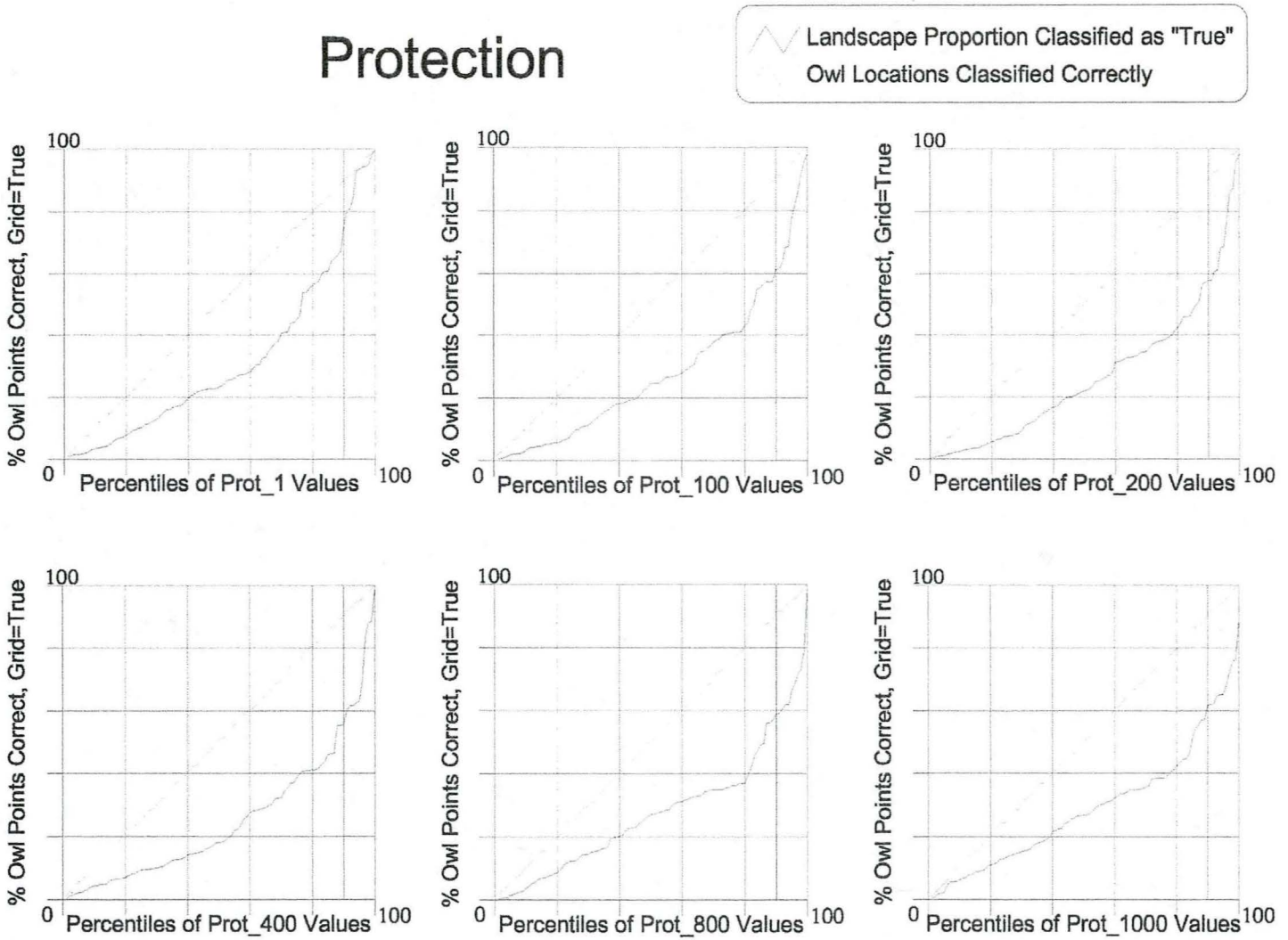

Figure 10: Proportions of the landscape corresponding with percentile ranges of Protection values, at 6 spatial scales.

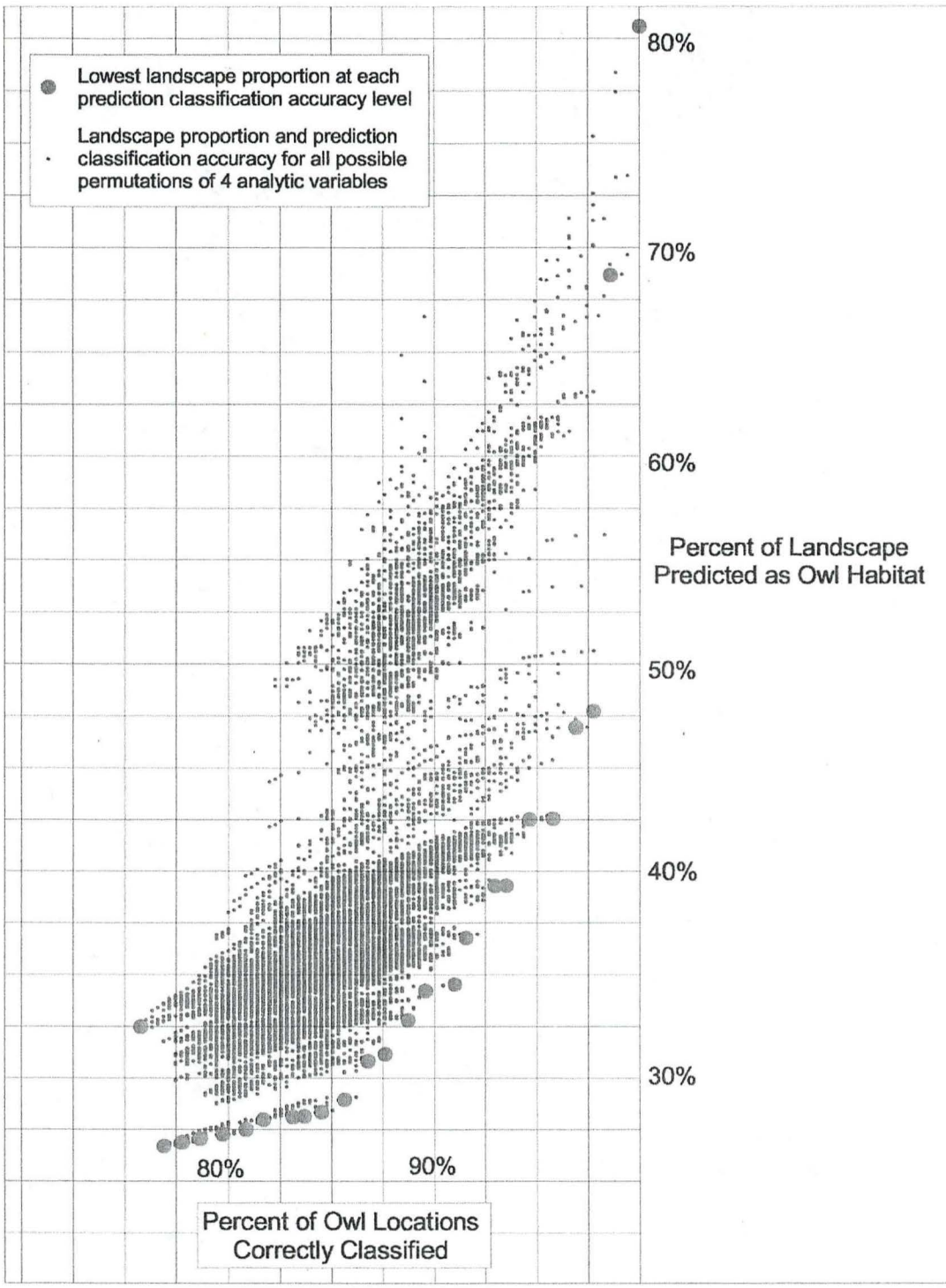

Figure 12: Landscape proportion and predictive accuracy for all possible combinations of Elevation, Slope, Surface Ratio and Protection layers in which the individual layer predicted ≥ 90% of the owl locations correctly.

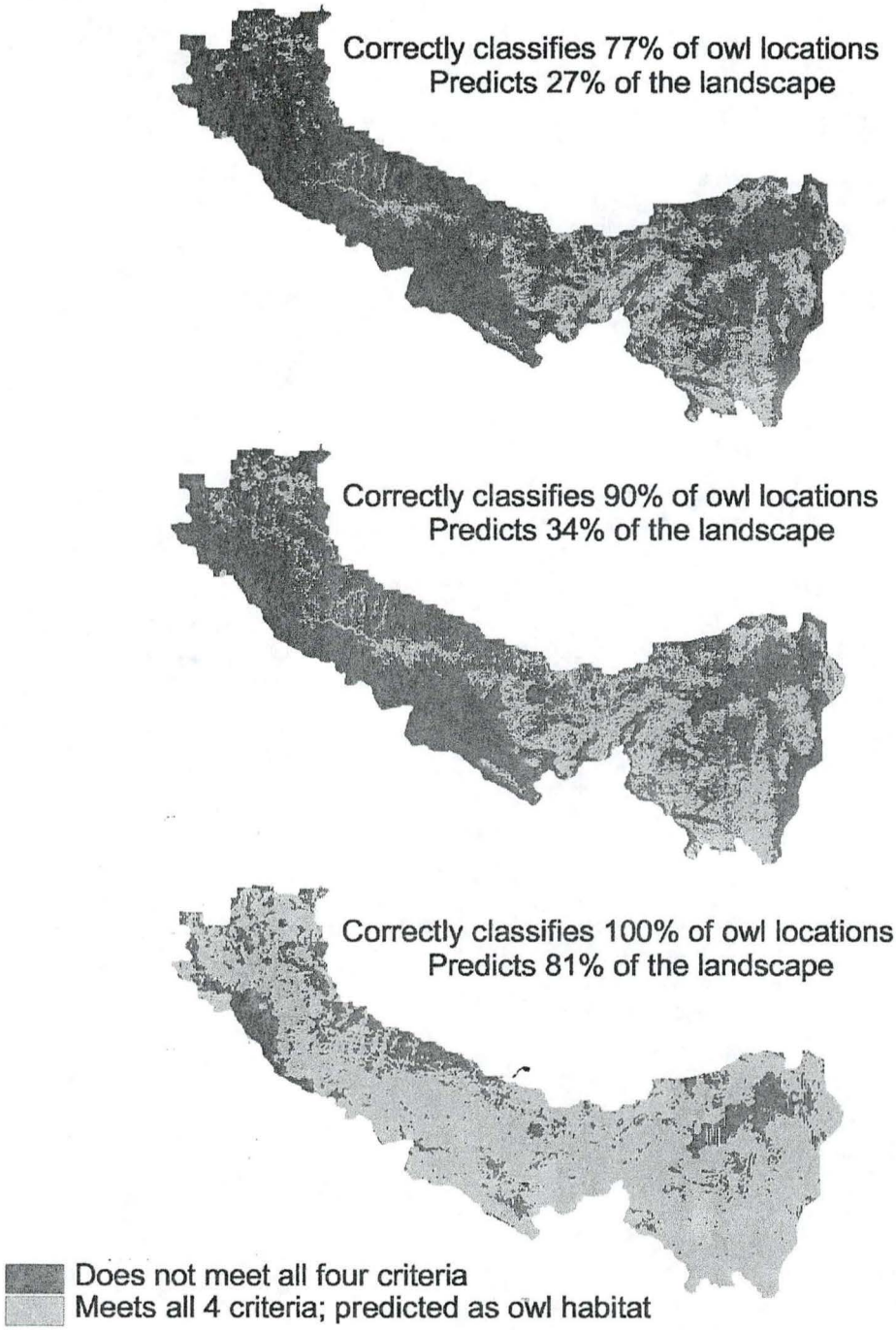
Correctly classifies 77% of owl locations
Predicts 27% of the landscape
Correctly classifies 90% of owl locations
Predicts 34% of the landscape
Correctly classifies 100% of owl locations
Predicts 81% of the landscape
Does not meet all four criteria
Meets all 4 criteria; predicted as owl habitat

Figure 13: Three of the 25 best models, illustrating the actual landscape predicted to be owl habitat when 77%, 90% and 100% of the owl locations are predicted accurately.